Urol Res (2012) 40:1–15
DOI 10.1007/s00240-011-0423-5

ORIGINAL PAPER

The effect of intracrystalline and surface-bound osteopontin on the degradation and dissolution of calcium oxalate dihydrate crystals in MDCKII cells

Lauren A. Thurgood · Esben S. Sørensen · Rosemary L. Ryall

Received: 22 March 2011 / Accepted: 22 August 2011 / Published online: 20 September 2011

Abstract In vivo, urinary crystals are associated with proteins located within the mineral bulk as well as upon their surfaces. Proteins incarcerated within the mineral phase of retained crystals could act as a defence against urolithiasis by rendering them more vulnerable to destruction by intracellular and interstitial proteases. The aim of this study was to examine the effects of intracrystalline and surface-bound osteopontin (OPN) on the degradation and dissolution of urinary calcium oxalate dihydrate (COD) crystals in cultured Madin Darby canine kidney (MDCK) cells. [^{14}C]-oxalate-labelled COD crystals with intracrystalline (IC), surface-bound (SB) and IC + SB OPN, were generated from ultrafiltered (UF) urine containing 0, 1 and 5 mg/L human milk OPN and incubated with MDCKII cells, using UF urine as the binding medium. Crystal size and degradation were assessed using field emission scanning electron microscopy (FESEM) and dissolution was quantified by the release of radioactivity into the culture medium. Crystal size decreased directly with OPN concentration. FESEM examination indicated that crystals covered with SB OPN were more resistant to cellular degradation than those containing IC OPN, whose degree of disruption appeared to be related to OPN concentration. Whether bound to the crystal surface or incarcerated within the mineral interior, OPN inhibited crystal dissolution in direct proportion to its concentration. Under physiological conditions OPN may routinely protect against stone formation by inhibiting the growth of COD crystals, which would encourage their excretion in urine and thereby perhaps partly explain why, compared with calcium oxalate monohydrate crystals, COD crystals are more prevalent in urine, but less common in kidney stones.

Keywords Osteopontin · Calcium oxalate dihydrate (COD) · Intracrystalline protein · Surface-bound protein · MDCKII cells · Urolithiasis

L. A. Thurgood · R. L. Ryall (✉)
Urology Unit, Department of Surgery, Flinders Medical Centre, Flinders University, Bedford Park, SA 5042, Australia
e-mail: rose.ryall@flinders.edu.au

L. A. Thurgood · R. L. Ryall
Flinders Clinical and Molecular Medicine, School of Medicine, Flinders University, Bedford Park, SA 5042, Australia

E. S. Sørensen
Protein Chemistry Laboratory, Department of Molecular Biology, Aarhus University, Aarhus, Denmark

Introduction

Provided they are expelled in the urinary stream, calcium oxalate (CaOx) and calcium phosphate (CaP) crystals resulting from excessive supersaturation are little more than harmless curiosities. In contrast, their retention within the kidney tubules (intratubular nephrocalcinosis) or renal interstitium (interstitial nephrocalcinosis) is regarded as an obligate forerunner to the formation of most kidney stones [1, 2]. Intratubular nephrocalcinosis, which is a consistent feature of experimental hyperoxaluric animals [3], has been observed in renal biopsies of brushite stone formers [4], and in individuals who have undergone bowel resection [5] and bariatric bypass surgery [6]. They also occur in preterm infants, patients with transplanted kidneys and those suffering from acute phosphate nephropathy and primary hyperoxaluria [7, 8]. Although intratubular CaOx crystals have recently been reported to be absent from renal biopsies of idiopathic stone formers, which are instead more commonly associated with interstitial nephrocalcinosis in

the form of Randall's plaque [9], their presence in the renal tubules of healthy subjects and stone formers has previously been demonstrated by a number of authors [10–13].

Mechanical obstruction of renal tubules with large or aggregated crystals could therefore be a major step in the formation of many CaOx kidney stones. The kidney, however, possesses several mechanisms for minimising the likelihood that crystals will adhere to the tubular epithelium [1, 14–18]. Numerous studies [reviewed by 19, 20] have demonstrated that macromolecular urine fractions and urine itself can reduce the ability of calcium oxalate monohydrate (COM) crystals to interact with and bind to cultured renal epithelial cells. Some specific proteins and glycosaminoglycans have been shown to have similar properties, including crystal adhesion inhibitor [21], osteopontin (OPN) [22] heparan sulphate [22] chondroitin sulphate A and B [22], chondroitin sulphate C [23], Tamm Horsfall glycoprotein [23], transforming growth factor β-2 [24], fibronectin [25], bikunin [26], and hepatocyte growth factor [27].

It is also apparent from in vitro cell culture work, as well as in vivo studies of humans and animals, that the kidney possesses other protective devices for preventing progression from crystal nucleation to urolithiasis. The intact, fully differentiated healthy tubular epithelium is impervious to crystal attachment, a property lost during cell proliferation or following injury [14, 26–28], which exposes underlying crystal-binding molecules, prominent among which are hyaluronic acid [14, 26, 29], CD44 antigen [14, 28] and OPN [14, 28–32]. Other binding molecules include nucleolin-related protein [33], annexin II [34], collagen IV [35, 36], collagen I and fibronectin [37], sialic acid [36, 37] and phosphatidylserine [36].

Although active attachment of crystals to the renal epithelium is regarded as one essential step in stone formation, it may also constitute an alternative means of defence against the disease. In lithogenic animal models, crystals attached to the tubular apical cell surface are overgrown by adjacent epithelial cells and actively transported to the interstitium [3, 8, 38, 39], a process originally called *exotubulosis* [38, 39], but more recently described as *transcytosis* [1]. It is also evident that epithelial overgrowth and transport of retained crystals occur in selected humans [8, 40, 41]. Once in the interstitium, crystals are encapsulated and disintegrated by macrophages and multinucleated giant cells [1, 40–42]. Similar observations have been reported in vitro. COM crystals attach to cultured cells, but are then phagocytosed and subsequently dissolved within the cytoplasm [22, 41, 43–49], a process that can take up to 7 weeks in renal epithelial cells [22, 47, 48], but only 4 days in macrophages [41].

Paradoxically, therefore, retention of crystals within the renal tubules may protect against calculus formation by enabling removal of intratubular crystals, as well as their destruction within the cytoplasm or interstitium, and it has been suggested that that stone pathogenesis may result from a defect in this process [50, 51]. Thus, any factor that increases the rate of crystal dissolution has the potential to retard progression from crystal nucleation to stone formation. Calcium oxalate crystals formed in urine are impregnated with proteins [52–54], which decrease the size of their crystallites and destabilize the mineral integrity by creating lattice discontinuities [54]. Such intracrystalline proteins have been shown to accelerate the gross physical degradation [44, 45] and dissolution [45] of urinary COM crystals within cultured renal cells, in proportion to their abundance within the mineral phase [45]. Although several studies have shown that calcium oxalate dihydrate (COD) crystals bind to cultured renal epithelial cells [22, 50, 55–57], only two have investigated their dissolution or degradation [56, 58]. One of these [58] observed that urinary COD crystals were less susceptible than urinary COM crystals to extracellular proteolytic degradation, while the other reported that inorganic COD crystals take several weeks to dissolve inside BSC1 cells [56]. It is well established that OPN is a consistent component of COD crystals formed in human urine [53, 59–61] and that it may play a crucial role in calcium stone formation. The protein is present in Randall's plaque [4], is an efficient inhibitor of COM crystallization in inorganic media [62–64] and of COD crystal growth in urine [65], and appears both to inhibit and mediate the attachment of COM [17, 66] crystals to renal epithelial cells. It also promotes COM crystal formation [67, 68] and attachment [14, 29] in experimental animals in vivo. Although OPN has been shown to influence the attachment of urinary COD crystals to cultured epithelial cells [65], its effect on their intracellular dissolution and physical decomposition has not previously been studied. In vivo, urinary crystals are associated with proteins located within the mineral bulk as well as upon their surfaces. The aim of the work reported here was to examine the degradation and dissolution of urinary COD crystals associated with intracrystalline (IC) and surface-bound (SB) OPN, as well as a combination of both (SB + IC), in cultured Madin Darby canine kidney (MDCK) cells.

Materials and methods

This study was reviewed and approved by the Flinders Clinical Research Ethics Committee.

All materials used were of analytical grade, unless otherwise mentioned. All solutions were prepared with high quality water from a "Hi Pure" water purification system (Permutit Australia, Brookvale, NSW, Australia).

Purification of OPN from human milk

OPN was purified from human milk [69] from a pool of donors as detailed in Christensen et al. [70]. SDS–PAGE and N-terminal sequencing verified that the final OPN preparation was of very high purity (>98%) [60]. The protein was dissolved in water for addition to the urine samples.

Preparation of urine samples

Fresh urine samples collected from healthy donors (3 females, 2 males) were shown to be free of blood and nitrites by dipstick analysis (Combur^7 Test®, Roche Diagnostics). They were pooled and centrifuged at 20°C and 10,000×*g* for 30 min (J2-21 M/E, Beckman Instruments, Fullerton, CA, USA), filtered through a 0.22 μm filter (GVWP14250, Millipore Corporation, Billerica, MA, USA), and then ultrafiltered (UF) using a PrepScale Spiral Wound TFF cartridge (Millipore Corporation, Bedford, MA, USA) with a nominal molecular weight cut-off of 10 kDa. The calcium concentration was determined by the *O*-cresophthalein complexone technique using an automated biochemical analyser and then adjusted to 8 mM by the addition of aqueous calcium chloride (1 mol/L) to ensure the nucleation of COD crystals [53]. [^{14}C]-oxalic acid (NEN Products, Boston MA, USA) was added to give a final radioactivity concentration of 3.125 μCi per 100 mL and the urine specimen was then divided into separate samples, which were treated to prepare different COD crystals as follows.

Crystals with intracrystalline OPN: IC crystals

The UF sample was divided into three aliquots to which OPN was separately added to give final concentrations of 0, 1.0 and 5.0 mg/L, which encompasses the published range of urinary OPN concentrations, namely, from 0.01 mg/L [71] to ~6 mg/L [72]. The metastable limit was measured and crystals were precipitated by the addition of a standard oxalate load as described previously [55, 73].

Crystals with surface-bound OPN: SB crystals

Crystals were precipitated from individual aliquots of the original UF urine sample containing no added OPN. After incubation for 2 h, OPN was added to the flask to give final concentrations of 0, 1.0 and 5.0 mg/L, and the incubation was extended for a further 1 h to allow the added OPN to adsorb to the crystal surfaces.

Crystals with intracrystalline and surface-bound OPN: IC + SB crystals

Precipitation was induced identically as described for crystals containing IC OPN. One hour after addition of the oxalate load, additional OPN was added to each flask to give the same concentration as was used at the start, and incubation was continued at 37°C for a further 1 h to allow the added OPN to adsorb to the crystal surfaces.

All the crystals were washed gently with distilled water, lyophilized, and stored at −70°C. Crystal suspensions were prepared by mixing the desired weight of crystals in UF urine at a suspension density of 400 μg/mL. They were sterilized by 3 × 20 min exposures to UV light in a Biological Safety Cabinet Class II (Email Air Handling, Australia).

SDS–PAGE and western blotting analyses were not performed on the crystals because of a lack of sufficient material, but also because we have previously confirmed that OPN is incorporated into urinary COD crystals [53, 60] in amounts directly proportional to the ambient protein concentration [53].

Cell culture

Type II Madin–Darby canine kidney cells (MDCK-II), were generously supplied by the late Dr Carl Verkoelen (Erasmus University, Rotterdam, The Netherlands). These cells were selected because they are robust, bind and internalise COM crystals without the need to inflict injury [74] and have been used in numerous studies of crystal–cell interactions [e.g., 22, 26, 34, 45, 75]. The cells were seeded onto 35 mm plastic plates and left to grow for 2 days at a density of 1 × 10^6 in Dulbecco's Modified Eagle's Medium (DMEM: Invitrogen) containing 10% fetal calf serum (FCS: Invitrogen). On day 2 the medium was removed and replaced with DMEM containing 0.5% FCS, and the cells were left for a further 24 h.

The culture medium was removed by aspiration, and the cells rinsed with 2 mL of phosphate-buffered saline (PBS: 10 mM Na_2PO_4, 155 mM NaCl, and 5.4 mM KCl, pH 7.4), saturated with CaOx. 1 mL of the CaOx-saturated PBS and 1 mL of the crystal suspension (400 μg/mL) were added to the 35 mm dish and gently agitated. The dishes were incubated at 37°C in a humidified incubator (5% CO_2–95% air) for 60 min to allow for crystal binding. This binding time was selected as most crystals had bound by 60 min and binding had stabilised by that time [65]. Unbound crystals were removed by aspiration and the cells were washed three times with 2 mL of filtered sterile CaOx saturated PBS. 3 mL of DMEM containing 0.5% FCS was added to the culture dish, which was left in an incubator (37°C, 5% CO_2) for the following times: 1, 2, 4, 6, 8 and

10 days. Culture medium was refreshed every 2 days to ensure maintenance of metabolic activity and to avoid accumulation of calcium and oxalate ions, which would raise the degree of CaOx supersaturation of the medium and prevent further dissolution [45]. Cells tolerated the crystals well as they did not appear to detach from the monolayer, which accorded with previous studies [44, 45] showing that MDCKII cells exposed to urinary COM crystals remain viable for long periods of time. Semangoen et al. [57] also reported that incubation of MDCK cells with 100 μg/mL of COD for 48 h did not increase cell death.

After the cells had been incubated for the desired time, they were rinsed three times with 2 mL of CaOx-saturated PBS. 1 mL of PBS and 0.5 mL of concentrated HCl were applied to each dish, and the cells and crystals were detached using a cell scraper. 600 μL of each cell suspension was added to a scintillation vial containing 4 mL of Beckmann ReadySafe® and counted in a liquid scintillation counter (Beckman LS 3801 Liquid Scintillation System).

Field emission scanning electron microscopy

The crystal suspensions were sonicated to disrupt any aggregates and filtered onto 13 mm nucleopore filters (SPI supplies, West Chester, PA, USA). Samples were coated with platinum to a thickness of 3 nM and examined using a Phillips XL30 field emission gun scanning electron microscope (FESEM). All samples were analysed using an accelerating voltage of 10 kV and spot size of 3. Crystal size was calculated from measurements of the length of one of the four equivalent {110} edges of each of 10 single crystals in 10 randomly selected fields. Values therefore represent the mean of 100 separate measurements.

Calculation of total crystal surface area

To calculate the total surface area of the COD crystals applied to the cells, the mean volume of the crystals was calculated from measurements of the {110} crystal edges using the formula for the volume of a regular tetrahedral bipyramid (octahedron), $V = 1/3\sqrt{2}.l^3$, where l, the length of each side. The densities of the COD crystals were assumed to be constant, even though they would have decreased slightly with increasing OPN concentration [76]. From the density of COD (1.94×10^{-6} μg/μm^3) and the mean crystal volume, the mass of a single crystal was calculated. From the total crystal mass applied (400 μg), the number of crystals was calculated, which was then used to determine the total surface area of all crystals applied.

Calculation of dissolution

Following the 60 min binding period, at time 0 the culture medium was removed from each dish by aspiration and the attached crystals dissolved by adding 1 mL of PBS followed by 0.5 mL of concentrated HCl. The cells were dislodged using a scraper. The solution was centrifuged and 600 μL of the supernatant was added to 4 mL ReadySafe® scintillation fluid to give the maximum counts attached to the cells at the start of the experiment. To determine dissolution for the remainder of the experiment, the medium was removed by aspiration at 1, 2, 4, 6, 8 and 10 days and counted as described. The percent dissolution of each was calculated from the counts per minute in the supernatant, relative to those at time 0, as previously described [45]. Values were not corrected for dissolution caused by the culture medium alone [77], because it is minor in comparison to that occurring in MDCKII cells [45].

Factors influencing crystal dissolution: the expression of experimental data

All other factors being equal, dissolution of crystals immersed in a solvent such as intracellular fluid must be a direct function of the crystal surface area accessible to the solvent. In this study, dissolution was quantified as the radioactivity released into the cell culture medium relative to the total radioactivity contained in the crystals bound to the cells at zero time. However, as reported previously [65], OPN significantly reduced the sizes of the precipitated crystals in a dose-dependent manner in the order $0 > 1 > 5$ mg/L. Given this disparity in crystal size, prima facie, it would seem intuitively logical to correct % radioactivity released for differences in surface area between the crystals generated at the three OPN concentrations. However, identical amounts (400 μg) of each type of crystal were applied to the cells. For all crystal types, therefore, the amount of radioactivity released into the medium must reflect not only the fraction of crystal mass that had dissolved, but exactly the same fraction of crystal volume, crystal number and crystal surface area, as pointed out by Wang et al. [55]. Thus, for a population of uniformly shaped crystals, dissolution can be validly quantified simply as % radioactivity released into the medium, relative to that bound to the cells at zero time, without correcting for any differences in surface area.

Under inorganic conditions, smaller crystals containing no protein should dissolve faster than larger crystals devoid of protein, because of their greater surface area to mass ratio. In vivo, however, crystal dissolution would be a function of several additional factors. First, the sizes of

COD crystals precipitated in the urinary tract would be inversely proportional to the ambient OPN concentration: that is, the higher the OPN concentration, the smaller would be the precipitated COD crystals, and the greater would be the amount of IC OPN relative to crystal mineral. Second, the IC OPN would be expected to disrupt the mineral continuity and destabilise the lattice [54], making the crystals more susceptible to comminution, which in turn would enlarge the surface area of mineral exposed to the surrounding fluid and increase the dissolution rate. Finally, proteases in the surrounding medium would be expected to degrade the protein, which would expose a greater surface area of mineral to the surrounding fluid and also increase the rate of mineral dissolution.

In vivo and in vitro, ambient OPN will unavoidably affect both crystal size and IC OPN content: alterations cannot occur in one without changes also occurring simultaneously in the other. Thus, the rate and extent of dissolution of COD crystals under physiological and experimental conditions will, by necessity, reflect the net result of both factors occurring concurrently, making it impossible to distinguish between any separate effects that either might have on crystal dissolution. Therefore, the release of ^{14}C-oxalate into the cell culture medium can be regarded as approximating the extent of dissolution that would be expected to occur in vivo, since it represents the combined effects of ambient OPN concentration, crystal size and IC OPN content. This does not, however, allow determination of the effects of OPN on crystal dissolution, separate from those of crystal size.

The cell culture model used in this study, though unable to reproduce physiological conditions faithfully, does at least provide an opportunity to estimate the effect of IC OPN on the extent and/or rate of COD crystal dissolution. In the experimental system used here, it is impossible to precipitate from the same urine specimen COD crystal populations of the same size, which also have different IC OPN concentrations. Equally, it is impossible to prepare COD crystals with different sizes, which also have identical IC OPN concentrations. However, by knowing the average surface area of crystals precipitated in the presence of different OPN concentrations, it is possible to obtain an indirect estimate of the influence of IC OPN on crystal dissolution by correcting measured rates or extents of dissolution for the total average surface area of the crystals applied to the cells.

Presentation of dissolution data

It should be stressed that the crystals used to test the effects of SB OPN were identical, so that corrections for surface area were not required. Those data are expressed simply in terms of %^{14}C-oxalate released into the medium.

On the basis of the foregoing discussion, the data obtained using the crystals associated with IC and IC + SB OPN are presented in two ways:

1. The amount of ^{14}C-oxalate released into the cell culture medium after a given period of time, expressed as a percentage of counts attached to the cell monolayer at zero time, is presented as being illustrative of the combined effects of crystal size and IC OPN concentration of OPN on crystal dissolution. These results provide an approximate assessment of the effects of OPN on crystal dissolution that would be expected to occur under physiological conditions.
2. The amount of ^{14}C-oxalate released into the cell culture medium after a given period of time, expressed as a percentage of counts attached to the cell monolayer at zero time and corrected for the total average surface area of the crystals, is presented as being indicative of any substantive effect of the IC OPN content on crystal dissolution.

Presentation of the data in these two ways makes certain assumptions:

- The IC concentration of OPN is directly proportional to the concentration of OPN in the urine from which the crystals were precipitated. This is supported by results of studies performed with unfractionated demineralised COM crystal extracts [45, 53, 78]. It is also corroborated by unpublished observations from our laboratory showing that the PTF1 content of urinary COM crystals increases in direct proportion to the concentration of protein in the ultrafiltered urine from which they are precipitated.
- The surfaces of all crystals are completely exposed to the surrounding cellular fluid. This may not have been the case, since some crystals, such as those shown in the scanning electron micrographs at 24 h, were not internalised into the cells, but remained upon the cell monolayer.

Additionally, under highly controlled and defined experimental conditions it would be strictly appropriate to apply a shrinking core model [79] to the data. However, that approach was impossible to adopt here, given the complexity of the physical and chemical environment surrounding the crystals, as well as physiological variations in the cells themselves.

Qualitative assessment of crystal degradation

A total of six 35 mm culture dishes, each containing a single 13 mm Thermanox Plastic coverslip (Nalge Nunc, Thermo Fisher Scientific, Rochester, NY, USA), were processed as described above, except that the retained crystals and cells were not detached from the dish. Instead,

at 24 h and 6 days at each OPN concentration (0, 1 and 5 mg/L), the coverslip was removed, lightly washed with CaOx-saturated PBS and mounted onto an aluminium stub, dried overnight at 37°C and coated with 3 nM platinum before being examined by FESEM as detailed above.

Statistical analysis

Binding and dissolution experiments were performed in triplicate and two aliquots were removed from each culture dish, giving a total of six values for each time point. Results are the average of two experiments conducted at different times; therefore all graph points represent the average of 12 different readings. A Mann–Whitney *U* test was used to compare values obtained for individual concentrations at specific time points and to compare the overall differences between the curves. In all cases, *P* values ≤ 0.05 were considered significant. All statistical comparisons were performed using SPSS Statistics 17.0 software.

Results

The average sizes of the crystals precipitated in the presence of 0, 1 and 5 mg/L OPN, expressed as the lengths of the {110} edges, were 21.9, 19.3 and 16.5 μm, respectively. The corresponding calculated mean crystal surface areas were 1661.4, 1290.3 and 943.1 μm^2. The incorporation of OPN into the COD crystals therefore caused a ~43% decrease in crystal size and a ~43% decrease in crystal surface area from the control crystals to those containing 5 mg/L of OPN. When the total surface area of all crystals applied to the cell monolayer was calculated, the larger control crystals had a much smaller total surface area (0.66 cm^2) compared to those containing 1 mg/L OPN (0.80 cm^2) and 5 mg/L (0.92 cm^2). Those values were multiplied by 1.5152 to give relative total surface areas of 1, 1.212 and 1.394 cm^2, in order to avoid obtaining values greater than 100% when data were corrected for total crystal surface area. Corrected data are therefore labelled on Figs. 3 and 5 as 'relative dissolution'.

Dissolution of COD crystals with SB OPN

The effects of SB OPN on crystal dissolution are presented in Fig. 1. At a concentration of 5 mg/L OPN strongly inhibited crystal dissolution, with ^{14}C-oxalate release reaching ~17% by day 2, but not increasing appreciably thereafter. Dissolution of crystals coated with 1 mg/L OPN continued throughout the entire 10 day period, reaching ~60% by 10 days, and following a pattern similar to that of the control crystals, which had dissolved by 75% at that time. Overall, all curves differed significantly from each other: 0 versus 1 mg/L ($P < 0.05$); 0 versus 5 mg/L ($P < 0.005$); 1 versus 5 mg/L ($P < 0.005$). Values at all individual time points differed significantly between the OPN concentrations, except for 0 versus 1 mg/L at days 1 and 4.

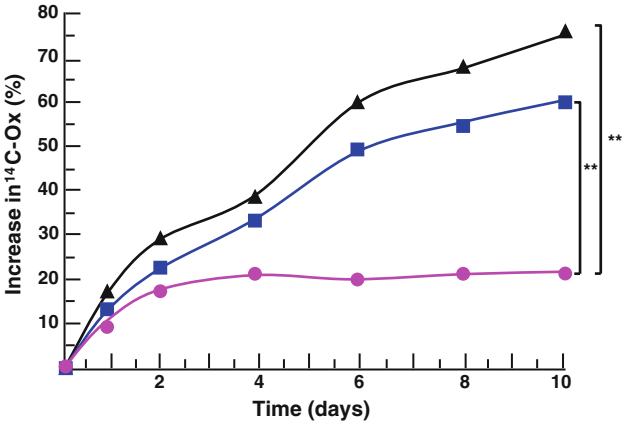

Fig. 1 Dissolution of COD crystals with different amounts of SB OPN, from 24 h until day 10 in MDCKII cells. *Error bars* have been omitted for the sake of clarity. Day 1: 0 versus 1 mg/L (NS), 0 versus 5 mg/L ($P < 0.05$), 1 versus 5 mg/L ($P < 0.05$); day 2: 0 versus 1 mg/L ($P < 0.05$), 0 vs 5 mg/L ($P < 0.05$), 1 versus 5 mg/L ($P < 0.05$); day 4: 0 versus 1 mg/L ($P < 0.05$), 0 versus 5 mg/L ($P < 0.05$), 1 versus 5 mg/L ($P < 0.05$); day 6: 0 versus 1 mg/L ($P < 0.05$), 0 versus 5 mg/L ($P < 0.05$), 1 versus 5 mg/L ($P < 0.05$); day 8: 0 versus 1 mg/L ($P < 0.05$), 0 versus 5 mg/L ($P < 0.05$), 1 versus 5 mg/L ($P < 0.05$); day 10: 0 versus 1 mg/L ($P < 0.05$), 0 versus 5 mg/L ($P < 0.05$), 1 versus 5 mg/L ($P < 0.05$). Curves were drawn by eye. Key: ▲ 0 mg/L, ■ 1 mg/L, ● 5 mg/L. Significant differences in the overall binding between each concentration up to day 10 are indicated as follows: *$P < 0.05$, **$P < 0.005$

Dissolution of COD crystals containing IC OPN: uncorrected

Figure 2 shows the release of ^{14}C-oxalate into the culture medium for crystals containing IC OPN, uncorrected for differences in total crystal surface area. By day 10, crystals with no added protein had dissolved by ~90%, while >70% of the mineral content of those with 1 and 5 mg/L had been released into the medium. There were statistically significant differences between dissolution values at some individual time points, namely between 0 and 1 mg/L at days 1 and 10; 0 and 5 mg/L at days 1, 2 and 10; and 1 and 5 mg/L at days 4 and 6. Although the control crystals containing no OPN dissolved more slowly than those containing OPN at either 1 or 5 mg/L OPN by 24 h, the trend was not maintained beyond that time. Overall, there were no significant differences between any of the curves.

Dissolution of COD crystals containing IC OPN: corrected

As was observed with the uncorrected dissolution values, when data were corrected for differences in surface area, the

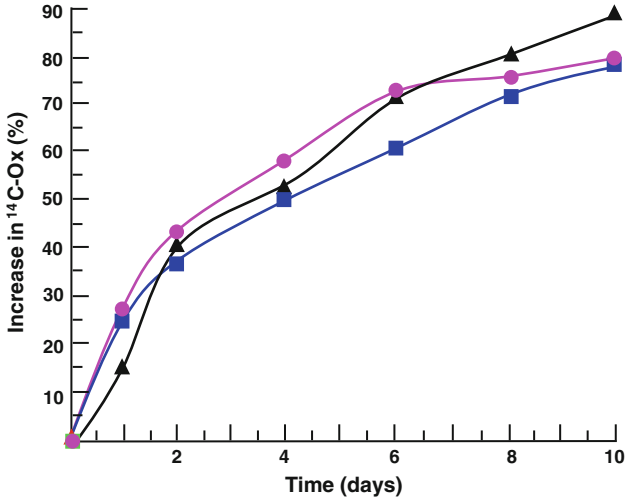

Fig. 2 Dissolution of COD crystals containing different amounts of IC OPN, from 24 h until day 10 in MDCKII cells. Values have not been corrected for differences in crystal surface area. *Error bars* have been omitted for the sake of clarity. Day 1: 0 versus 1 mg/L ($P < 0.005$), 0 versus 5 mg/L ($P < 0.005$), 1 versus 5 mg/L (NS); day 2: 0 versus 1 mg/L (NS), 0 versus 5 mg/L ($P < 0.005$), 1 versus 5 mg/L (NS); day 4: 0 versus 1 mg/L (NS), 0 versus 5 mg/L (NS), 1 versus 5 mg/L (NS); day 6: 0 versus 1 mg/L (NS), 0 versus 5 mg/L (NS), 1 versus 5 mg/L ($P < 0.005$); day 8: 0 versus 1 mg/L (NS), 0 versus 5 mg/L (NS), 1 versus 5 mg/L (NS); day 10: 0 versus 1 mg/L ($P < 0.05$), 0 versus 5 mg/L ($P < 0.05$), 1 versus 5 mg/L (NS). Curves were drawn by eye. Key: ▲ 0 mg/L, ■ 1 mg/L, ● 5 mg/L

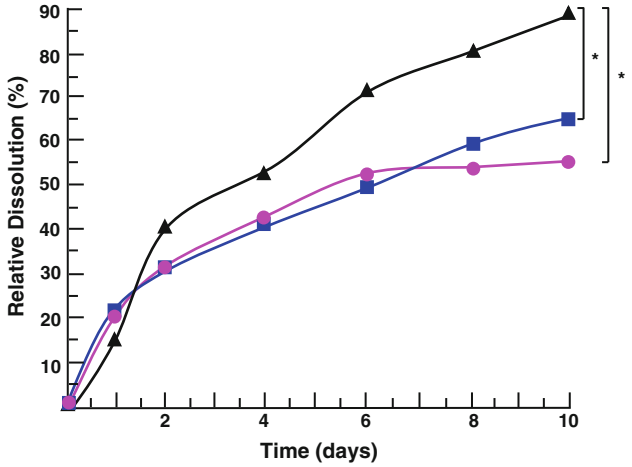

Fig. 3 Dissolution of COD crystals containing different amounts of IC OPN, from 24 h until day 10 in MDCKII cells. Values have been corrected for differences in total crystal surface area. *Error bars* have been omitted for the sake of clarity. Day 1: 0 mg/L versus 1 mg/L ($P < 0.05$), 0 versus 5 mg/L ($P < 0.005$), 1 versus 5 mg/L (NS); day 2: 0 versus 1 mg/L ($P < 0.05$), 0 versus 5 mg/L ($P < 0.005$), 1 versus 5 mg/L (NS); day 4: 0 versus 1 mg/L (NS), 0 versus 5 mg/L (NS), 1 versus 5 mg/L (P); day 6: 0 versus 1 mg/L ($P < 0.05$), 0 versus 5 mg/L ($P < 0.005$), 1 versus 5 mg/L (NS); day 8: 0 versus 1 mg/L ($P < 0.05$), 0 versus 5 mg/L ($P < 0.005$), 1 versus 5 mg/L (NS); day 10: 0 versus 1 mg/L ($P < 0.05$), 0 versus 5 mg/L ($P < 0.005$), 1 versus 5 mg/L ($P < 0.05$). Curves were drawn by eye. Key: ▲ 0 mg/L, ■ 1 mg/L, ● 5 mg/L. Significant differences in the overall binding between each concentration up to day 10 are indicated as follows: $*P < 0.05$, $**P < 0.005$

control crystals showed a slight initial lag at day 1 compared with those containing OPN (Fig. 3). However, after day 1 the control crystals consistently dissolved significantly more rapidly than those deposited in the presence of either 1 or 5 mg/L OPN. This was evident both for the individual values at each time point and also for the curves overall. However, there were no differences between corrected values for the crystals containing 1 and 5 mg/L OPN, except at day 10.

Dissolution of COD crystals with SB and IC OPN: uncorrected

Figure 4 shows the dissolution of crystals associated with both SB and IC OPN. Initial dissolution of the control crystals was indistinguishable from that of the 1 mg/L crystals, but remained lower at all times after day 2, reaching a maximum of ~63% ^{14}C-oxalate release by day 6 and remaining unaltered thereafter. Although the 5 mg/L crystals initially dissolved more rapidly than the others, after day 2 their dissolution was less than that of the 1 mg/L crystals, but greater than that of the controls, a pattern that persisted up to day 10. By day 10, dissolution of the crystals associated with both 1 and 5 mg/L OPN had stabilised to apparent maximum values of ~70%—only slightly greater than that of the control crystals. Overall, only the 0 and 1 mg/L curves differed significantly ($P < 0.05$). Nonetheless, there were significant differences between dissolution values at individual time points, as detailed in the legend to Fig. 4.

Dissolution of COD crystals with SB and IC OPN: corrected

Figure 5 shows the time course of dissolution, corrected for total crystal surface area. Apart from day 1, where values were indistinguishable, dissolution was slowest for the crystals associated with 5 mg/L OPN, rising to no more than 45% throughout the entire 10 day period. By comparison, relative dissolution of the control crystals rose continuously to reach ~65% at day 10. The 1 mg/L crystals followed a similar pattern to reach 60% at day 10. Overall, the control crystals dissolved significantly more rapidly than those associated with 1 and 5 mg/L OPN ($P < 0.005$), and the 1 mg/L crystals dissolved faster than the 5 mg/L crystals ($P < 0.05$). Moreover, other than those at day 1, individual corrected values at all time points differed significantly.

Qualitative assessment of crystal degradation

Figures 6, 7 and 8 show typical crystals attached to the cell monolayers at days 1 and 6. At day 6, few crystals were

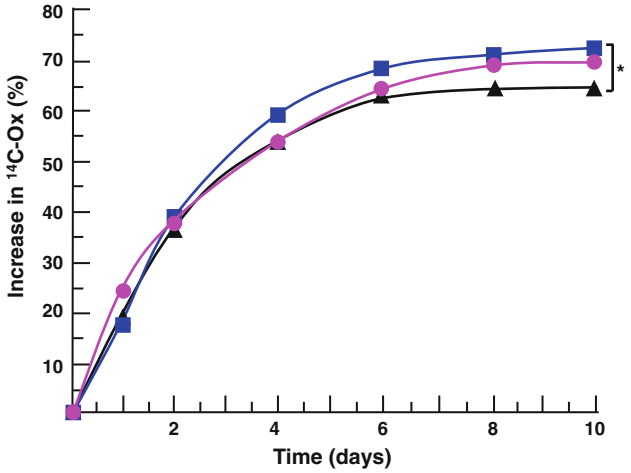

Fig. 4 Dissolution of COD crystals associated with different amounts of SB and IC OPN, from 24 h until day 10 in MDCKII cells. Values have not been corrected for differences in crystal surface area. *Error bars* have been omitted for the sake of clarity. Day 1: 0 versus 1 mg/L (NS), 0 versus 5 mg/L ($P < 0.005$), 1 versus 5 mg/L ($P < 0.05$); day 2: 0 versus 1 mg/L (NS), 0 versus 5 mg/L (NS), 1 versus 5 mg/L (NS); day 4: 0 versus 1 mg/L ($P < 0.05$), 0 versus 5 mg/L (NS), 1 versus 5 mg/L ($P < 0.05$); day 6: 0 versus 1 mg/L ($P < 0.05$), 0 versus 5 mg/L (NS), 1 versus 5 mg/L ($P < 0.05$); day 8: 0 versus 1 mg/L ($P < 0.05$), 0 versus 5 mg/L (NS), 1 versus 5 mg/L (NS); day 10: 0 versus 1 mg/L ($P < 0.005$), 0 versus 5 mg/L ($P < 0.05$), 1 versus 5 mg/L (NS). Curves were drawn by eye. Key: ▲ 0 mg/L, ■ 1 mg/L, ● 5 mg/L. Significant differences in the overall binding between each concentration up to day 10 are indicated as follows: *$P < 0.05$, **$P < 0.005$

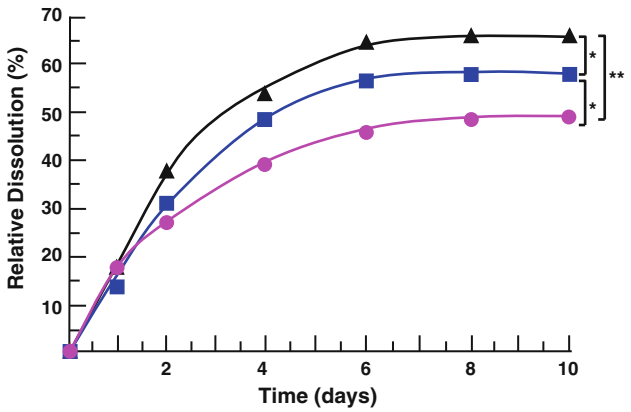

Fig. 5 Dissolution of COD crystals associated with different amounts of SB and IC OPN, from 24 h until day 10 in MDCKII cells. Values have been corrected for differences in crystal surface area. *Error bars* have been omitted for the sake of clarity. Day 1: 0 versus 1 mg/L (NS), 0 versus 5 mg/L ($P < 0.005$), 1 versus 5 mg/L (NS); day 2: 0 versus 1 mg/L ($P < 0.005$), 0 versus 5 mg/L ($P < 0.005$), 1 versus 5 mg/L ($P < 0.05$); day 4: 0 versus 1 mg/L ($P < 0.005$), 0 versus 5 mg/L ($P < 0.005$), 1 versus 5 mg/L ($P < 0.005$); day 6: 0 versus 1 mg/L ($P < 0.005$), 0 versus 5 mg/L ($P < 0.005$), 1 versus 5 mg/L ($P < 0.005$); day 8: 0 versus 1 mg/L ($P < 0.005$), 0 versus 5 mg/L ($P < 0.005$), 1 versus 5 mg/L ($P < 0.005$); day 10: 0 versus 1 mg/L ($P < 0.005$), 0 versus 5 mg/L ($P < 0.005$), 1 versus 5 mg/L ($P < 0.005$). Curves were drawn by eye. Key: ▲ 0 mg/L, ■ 1 mg/L, ● 5 mg/L. Significant differences in the overall binding between each concentration up to day 10 are indicated as follows: *$P < 0.05$, **$P < 0.005$

visible upon the cell monolayers, most having already been internalised: images presented for day 6 cannot therefore necessarily be regarded as representative of crystals at that time. Attempts to examine crystals at day 10 were unsuccessful, as by then they had all been internalised into the cells.

At day 1, crystals containing 1 and 5 mg/L IC OPN (Fig. 6) show slight surface degradation in the form of shallow depressions and pitting, while the control crystal is less affected. The larger pits in the 1 and 5 mg/L crystals probably represent voids left by removal of an interpenetrant twin crystal separated during sonication prior to application to the cells, rather than from cellular erosion. By day 6, however, all crystals show evidence of degradation and are closely associated with organic material, at least some of which (since it is evident in the control crystals) must have originated from the cells. Although the central region of the control crystal shown in Fig. 6 is relatively intact, its {110} edges are significantly eroded. The crystals containing OPN are more severely affected, particularly the 5 mg/L crystals, which shows a large void in its central region as well as what appear to be subcrystalline particles [52] that are also evident around the crystal's {110} edges. These may have been caused by leaching of IC OPN, as well as proteins with molecular masses <10 kDa.

The surfaces of crystals coated with SB OPN (Fig. 7) show relatively little surface damage at day 1, although there is some damage to the {110} edge of the control

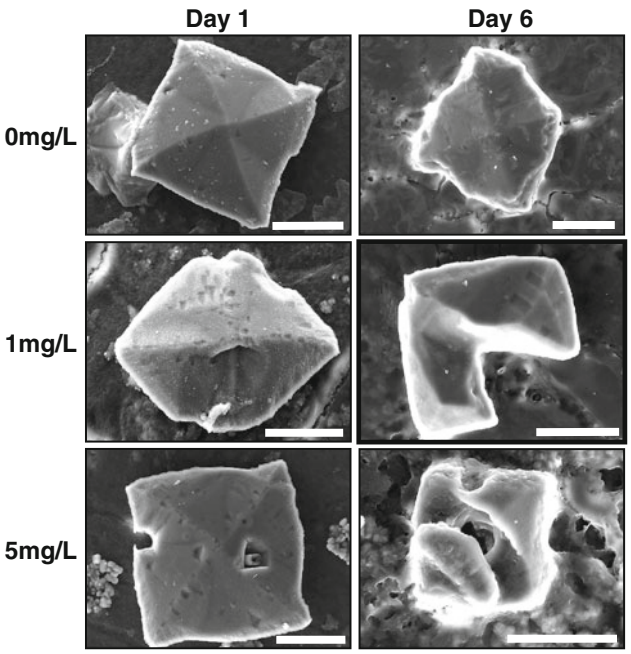

Fig. 6 FESEM images of COD crystals with intracrystalline OPN (0, 1 and 5 mg/L) at 1 day and 6 days after application to MDCKII cells. All *bars* represent 10 μm

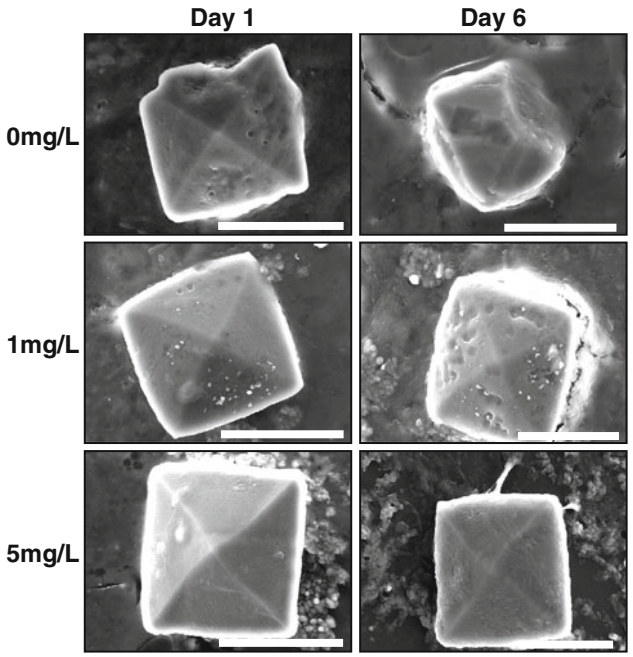

Fig. 7 FESEM images of COD crystals with OPN (0, 1 and 5 mg/L) bound only to their surfaces at 1 day and 6 days after application to MDCKII cells. All *bars* represent 10 μm

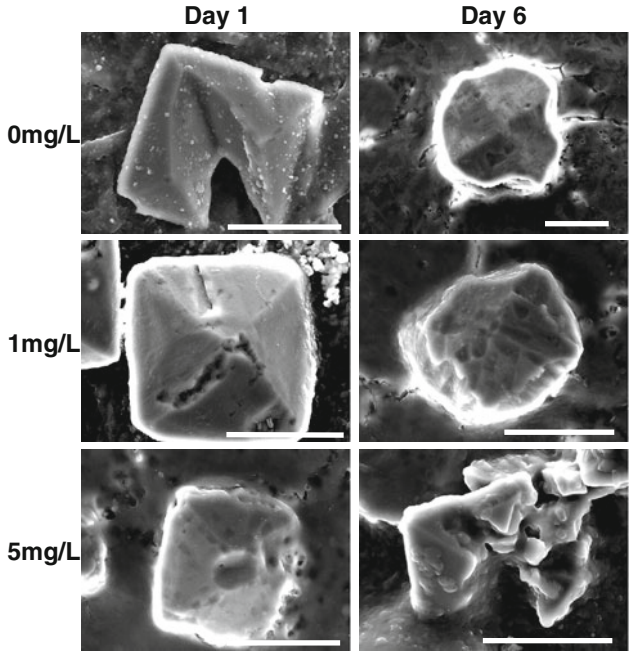

Fig. 8 FESEM images of COD crystals with intracrystalline OPN and also coated with the protein, at concentrations of 0, 1 and 5 mg/L at 1 day and 6 days after application to MDCKII cells. All *bars* represent 10 μm

crystal and minor disruption to two of the {101} surfaces. All crystals are associated with significant quantities of organic, presumably mainly cellular material. The 1 mg/L crystal shows some minor surface pitting, while the 5 mg/L crystal appears undamaged. By day 6, the bulk of the control crystal, which is partly submerged in the cell monolayer, is relatively intact, despite missing its top right hand corner, probably as a result of removal of an adjacent twin. The 1 mg/L crystal is covered with organic material, which appears incompletely to cover some surface pits located beneath. The 5 mg/L crystal, which is tethered to the monolayer by cell extensions, is relatively intact.

Figure 8 shows images of crystals with IC + SB OPN. At day 1, the control crystal contains a large void, which from its shape, probably resulted from removal of an interpenetrant twin crystal (see above). The surface of the 1 mg/L crystal, however, shows significant pitting, particularly along abutting edges of two of the {101} faces, which suggests removal of IC material. The 5 mg/L crystal, which is partly embedded within the cell monolayer is also pitted, the true extent of which appears to be partly concealed by abundant organic material spread over its surfaces. By day 6, all crystals show signs of significant decomposition, which in the control and 1 mg/L crystals appears to have advanced from the outer edges towards the crystal centres, which are relatively intact. On the other hand, the 5 mg/L crystal is severely degraded, partly comminuted, and closely associated with fragments. Internal sub-crystalline particles [52] are again evident.

Discussion

Interactions between crystals and cells involve interconnected steps, including initial crystal attachment, internalization (phagocytosis), physical disruption, and finally, dissolution [16], which presents a major challenge to studies designed to quantify the effects of macromolecules on each separate process. We recently reported that although OPN generally reduced the binding of urinary COD crystals to MDCKII cells, irrespective of whether it was intracrystalline or bound to the crystal surfaces, at times it also appeared to mediate adhesion [65]. However, the protein's effect on intracellular dissolution and physical decomposition of crystals has not previously been investigated. Under physiological conditions, COD crystals would contain OPN within their mineral phase, as well as attached to their surfaces. Thus, in this study the effects of SB and IC OPN, both separately and in combination, on the physical erosion and dissolution of COD crystals in MDCKII cells were investigated.

Crystal dissolution was quantified as the amount of radioactivity released into the cell culture medium. A limitation of this approach is that it relies on the assumption that once bound, crystals do not later detach. Using crystals identical to those used here, we have shown

previously [65] that attachment of crystals reaches a maximum by 60 min, which was the binding period used in the present study. Moreover, crystal internalization is rapid [44, 46]. It is therefore not unreasonable to assume that ^{14}C-oxalate released into the culture medium reflects release of ions from the mineral bulk, rather than dislodgement of loosely bound crystals. At concentrations of both 1 and 5 mg/L, SB OPN significantly inhibited the release of ^{14}C-oxalate into the cell culture medium at every time point, as well as overall. Inhibition was proportional to OPN concentration, since dissolution at 5 mg/L was consistently less than that at 1 mg/L. Furthermore, by day 4, dissolution of the 5 mg/L crystals had ceased completely, indicating that the OPN coating enabled the crystals to resist intracellular dissolution, even after 10 days. Analysis of these data was straightforward, since the crystals used were all derived from the same preparation, which obviated any need to correct for differences in total surface area. However, calculation and interpretation of dissolution data obtained from the crystals with IC and IC + SB OPN were more complicated because their sizes were not identical.

As reported previously [65] the mean size of the COD crystals precipitated from urine in the presence of OPN decreased indirectly with increasing OPN concentration, demonstrating that OPN inhibits COD crystal growth, and supporting previous observations with COM in inorganic solutions [62–64]. In the present study, because identical masses of each crystal type were applied to the cells, the total crystal surface area exposed to the surrounding environment would have increased directly with OPN concentration. Therefore, if crystal dissolution had been a function only of crystal size, logically, the rate of crystal dissolution would have been expected to rise relative to OPN concentration. However, the smallest crystals, which had the highest total surface area, contained the greatest amounts of OPN, and vice versa. Uncorrected dissolution rates of crystals containing IC OPN must therefore have reflected the net result of the protein's effect on surface area in addition to any substantive influence it might have had on crystal dissolution. Measurements of ^{14}C-oxalate released into the medium, corrected for differences in total crystal surface area, were therefore regarded as indicative of any direct effect of IC OPN on crystal dissolution.

At day 1, IC OPN appeared to facilitate crystal dissolution relative to the control, but this pattern was not maintained. Although significant differences between the control crystals and those containing the two IC OPN concentrations were observed at some individual time points, overall, dissolution did not differ significantly throughout the 10 day period. This finding strongly suggested that by inhibiting crystal dissolution, IC OPN had counteracted any expected increase in mineral dissolution produced by the corresponding reduction in crystal size. This was confirmed when the data were corrected for crystal surface area. Again, before 24 h IC OPN slightly, but significantly, increased the liberation of ^{14}C-oxalate, but this was reversed by day 2, after which individual values and the overall dissolution rates of both the 1 and 5 mg/L crystals were significantly depressed compared with the control crystals. These results confirmed that IC OPN decreased the rate of dissolution of urinary COD crystals in MDCKII cells, in keeping with the corresponding results for the crystals with SB OPN. Similar inhibition was also observed with the crystals with IC + SB OPN. After correction for differences in total surface area, after day 1 OPN significantly inhibited dissolution, both overall and at individual time points. Such differences were not observed when surface area was not taken into account. These results therefore demonstrated that OPN, whether located upon the crystal surface or incorporated within the mineral bulk, inhibited COD crystal dissolution in MDCKII cells.

Inhibition of dissolution by SB proteins seems intuitively logical, since they could physically shield the crystal surface from the surrounding environment. By blocking access of ambient solvent to component crystallites, IC proteins could also retard dissolution. Incorporation of proteins into mineral crystals markedly affects their physical and mechanical properties [80], including their solubility [81]. In aqueous EDTA, dissolution rates of COM crystals containing IC proteins are inversely related to the protein content [82], and under similar conditions, CaOx stone fragments dissolve significantly more slowly than do pure inorganic crystals [83]. However, controlled dissolution of crystals in an inorganic extracellular medium does not mimic the interior of renal epithelial cells, in which crystals would be exposed to proteolytic enzymes and the acidic environment of the phagolysosome. It has been hypothesised that under such circumstances, internalised crystals containing occluded proteins would be degraded by intracellular proteases and thus more likely to undergo comminution and dissolution [51, 52, 54]. Although this proposal is supported by one report showing that crystals containing mixed urinary proteins dissolved more rapidly in MDCKII cells than crystals lacking proteins [45], that study used urinary COM crystals. Under inorganic conditions, pure COD has a higher dissolution rate than pure COM [84]. It is likely, therefore, that our contrary findings with COD are related to differences between the protein content of the crystals used in each study.

The ability of cells to degrade and dissolve crystals containing IC proteins will rely, among other factors, on the ability of their component proteases to degrade the proteins associated with the crystals. As discussed above, if they cannot, dissolution is more likely to be retarded.

Urinary COD crystals precipitated from filtered human urine contain more proteins than COM [53, 61], but in the present study the COD crystals were precipitated from UF urine to which only OPN had been added. It is reasonable to suppose that crystals containing a wide variety of proteins would be more susceptible to degradation by cells containing a broad range of proteases. On the other hand, crystals containing only a single major protein that is not susceptible to attack by those proteases are less likely to undergo significant proteolytic erosion. MDCK cells express a variety of proteases with a broad scope of functions, including MMP-7 [85], carboxypeptidase M [86], leucine aminopeptidase [87, 88]; alkaline phosphatase [89], thimet-oligopeptidase [90], γ-glutamyl transpeptidase [87–89] as well as various unidentified metallo- and serine proteases [91]. They also express the lysosomal proteases cathepsins B, L, and D [90], acid phosphatase [87], *N*-acetyl glucosaminidase [87] and *N*-acetyl-β,D-hexosaminidase [88, 91]. Moreover, the activities of *N*-acetyl-β,D-hexosaminidase, γ-glutamyl transpeptidase and leucine aminopeptidase are raised in the culture medium of MDCK cells challenged with COM crystals [88].

Of the listed proteases, human OPN is cleaved by a lysosomal acid phosphatase [92], as well as cathepsin D and MMP [93], particularly MMP-3 and 7 [94]. It is also well known that the protein is degraded by thrombin [e.g., 93]; but although mRNA corresponding to the F1 region of prothrombin is present in MDCK cells [95], there have been no reports that they express functional thrombin. To our knowledge, there is no published information about the susceptibility of OPN to the remaining MDCK proteases mentioned in the previous paragraph. Unlike crystal dissolution, which we attempted to assess quantitatively, physical degradation can be evaluated only qualitatively. This was achieved using FESEM. From the results presented here, it would appear that superficially bound human OPN is not easily degraded by any of the proteases expressed in MDCKII cells since those crystals appeared to remain largely intact. However, crystals containing IC OPN were partly degraded, with clear evidence of superficial pitting and disruption to adjoining {101} faces, both of which were more extensive at the higher OPN concentration. Although these findings might suggest that crystals covered by OPN are more resistant to attack by intracellular proteases than are those containing intracrystalline protein, it must be stressed that attached crystals were directly observable only at day 1, at which time most appeared still to be located on the surface of the cell monolayer. However, internalisation of adherent COM crystals is relatively rapid [44, 46] and it is likely that COD crystals are also phagocytosed quickly, and by day 6, when the FESEM images were collected, very few crystals were still visible. By day 10, no crystals could be observed at all. Phagolysosomal degradation and dissolution of crystals must occur intracellularly and can be assessed directly only by the use of techniques such as transmission electron microscopy [e.g., 46] or confocal microscopy [e.g., 26]. Therefore, a limitation of the present investigation is that the physical features of the few crystals remaining upon the cell monolayer at day 6 are unlikely to be representative of the appearance of those inside the cells. It is likely that the observed degradation was caused by the action of proteases, some of which are known to be secreted into the culture medium by cells challenged with crystals [45]. This possibility could be tested directly in future studies using conditioned culture medium.

Nonetheless, the likelihood that COD crystals are resistant to proteolytic degradation is supported by the present observation that OPN significantly inhibited dissolution, as well as findings by others. Webber et al. [58] compared COD and COM crystals precipitated from the same urine and showed that COD crystals were more resistant to degradation by proteinase K, and also by cathepsin D, which is a lysosomal protease present in MDCK cells [90] and active throughout the tubules of the human nephron [96], and which is known to cleave OPN [93]. Interestingly, the COD crystals in that study were also resistant to erosion by thrombin, to which OPN is particularly sensitive [e.g., 93], and less susceptible to extracellular dissolution. Given the expression of a broad range of proteases by MDCK cells, the apparent resistance of IC and SB OPN to intracellular degradation is puzzling. However, there are a number of plausible explanations:

1. Human OPN cannot be cleaved by canine proteases. Wide interspecies differences exist in primary amino acid sequence [97] and post-translational modifications [98] that can affect the functions of the resulting OPN isoforms [98], and probably, therefore, their susceptibilities to enzymatic degradation.
2. Conformational modifications can result from formation of multiple bonds between proteins and surfaces [99]. Binding of OPN to the COD crystal surface may therefore change its configuration and conceal bonds normally accessible to enzymatic cleavage. The probability that OPN adopts different conformations and/or orientations when adsorbed to the COD crystal surface is strengthened by its sensitivity to cleavage by thrombin only when adsorbed to a hydrophobic surface [100].
3. MDCK cells express at least one unidentified protease inhibitor [101] and may also secrete others capable of inhibiting particular proteases to which OPN is otherwise sensitive.
4. Other cellular components may bind to OPN and mask bonds in the molecule that are vulnerable to proteases. Kon et al. [102] showed, for instance, that syndecan 4

protects against OPN-induced hepatotoxicity by masking functional domains on the OPN molecule.

5. Structural alterations to the OPN molecule, resulting either from its incorporation into the COD crystal mineral or the action of other MDCK enzymes might render the OPN molecule resistant to degradation by proteases to which it would otherwise be susceptible. For instance, alterations in OPN's sialic acid moieties can prevent its interaction with its cell surface receptor on transformed TSB77 cells [103].

It would appear that the majority of cells throughout the human nephron should be capable of proteolytic degradation of internalised crystals containing IC proteins, as proteases have been identified inside cells of the proximal tubules [96, 104], thick ascending limbs of Henlé [96], the basement membrane [105], the collecting ducts [106] and distal tubules [104]. MDCKII cells are characteristic of distal tubular cells [107]. This region of the human kidney contains small lysosomes whose predominant proteases are dipeptidylpeptidase I and cathepsin B [104], both of which are also found in the proximal tubules [104].

There is also other evidence that proteases are involved in urinary stone disease. Levels of the two traditional lysosomal enzyme markers, *N*-acetyl-β-glucosaminidase and β-galactosidase [108] and an unidentified serine protease that alters the excreted form of OPN [71], are raised in stone formers' urines, as are those of the brush border proteases α-glucosidase, angiotensin 1-converting enzyme and γ-glutamyltranspeptidase [109]. This suggests that the human nephron contains abundant proteases, which in combination with others secreted at the apical cell membranes could begin the digestion of urinary crystals as soon as attachment occurred.

However, at the present time there is no unequivocal evidence that renal proteases are involved in the putative dissolution of internalised COM or COD crystals in vivo. A major drawback of the present study, as with any based on cultured cells, and particularly those derived from other species, is that results do not necessarily translate to events that would occur under physiological conditions in the human kidney. Nonetheless, the work reported here at least provides some clue as to the possible influence of OPN on COD crystal dissolution following their internalisation by renal epithelial cells. Irrespective of the reasons for OPN's apparent insensitivity to enzymatic digestion, it is clear that whether bound to the crystal surface or incarcerated within the mineral interior, the protein inhibits the dissolution of COD crystals in MDCKII cells. Under physiological conditions, therefore, OPN may routinely contribute to the prevention of stone disease by inhibiting the growth of COD crystals in urine, as well as their binding to renal cells [65], which would encourage their excretion in urine and thereby perhaps at least partly explain why, compared with COM crystals, COD crystals are more prevalent in urine, but less common in kidney stones.

Acknowledgments Support from the National Institute of Diabetes and Digestive and Kidney Diseases (Grant 1R01-DK-064050-01A1), and Flinders Medical Centre Foundation and Volunteer Service is gratefully acknowledged.

References

1. Vervaet BA, Verhulst A, D'Haese PC, De Broe ME (2009) Nephrocalcinosis: new insights into mechanisms and consequences. Nephrol Dial Transpl 24:2030–2035
2. Coe FL, Evan AP, Worcester EM, Lingeman JE (2010) Three pathways for human kidney stone formation. Urol Res 38:147–160
3. Khan SR (1995) Experimental calcium oxalate nephrolithiasis and the formation of human urinary stones. Scan Microsc Int 9:89–101
4. Evan AP, Coe FL, Rittling SR, Bledsoe SB, Shao Y, Lingeman JE, Worcester EM (2005) Apatite plaque particles in inner medulla of kidneys of calcium oxalate stone formers: osteopontin localization. Kidney Int 68:145–154
5. Evan AP, Lingeman JE, Worcester EM, Bledsoe SB, Sommer AJ, Williams JC, Krambeck AE, Philips CL, Coe FL (2010) Renal histopathology and crystal deposits in patients with small bowel resection and calcium oxalate stone disease. Kidney Int 78:310–317
6. Evan AP, Coe FL, Gillen D, Lingeman JE, Bledsoe S, Worcester EM (2008) Renal intratubular crystals and hyaluronan staining occur in stone formers with bypass surgery but not with idiopathic CaOx stones. Anat Rec 291:325–334
7. Verhulst A, Asselman M, De Naeyer S, Vervaet BA, Mengel M, Gwinner W, D'Haese PC, Verkoelen CF, De Broe ME (2005) Preconditioning of the distal tubular epithelium of the human kidney precedes nephrocalcinosis. Kidney Int 68:1643–1647
8. Vervaet BA, Verhulst A, Dauwe SE, De Broe ME, D'Haese PC (2009) An active renal crystal clearance mechanism in rat and man. Kidney Int 75:41–51
9. Evan AP, Lingeman JE, Coe FL, Parks JH, Bledsoe SB, Shao Y, Sommers AJ, Paterson RF, Kuo RL, Grynpas M (2003) Randall's plaque of patients with nephrolithiasis begins in basement membranes of thin loops of Henle. J Clin Invest 111:607–616
10. Beer E (1904) Lime deposits especially the so-called "kalkmetastasen", in the kidney. J Pathol Bacteriol 9:225–233
11. Stout HA, Akin RH, Morton E (1955) Nephrocalcinosis in routine necropsies: its relationship to stone formation. J Urol 74:8–22
12. Bennington JL, Haber SL, Smith JV, Warner NE (1964) Crystals of calcium oxalate in the human kidney. Am J Clin Pathol 41:8–14
13. Ebisuno S, Kohjimoto Y, Tamura M, Inagaki T, Ohkawa T (1997) Histological observations of the adhesion and endocytosis of calcium oxalate crystals in MDCK cells and in rat and human kidney. Urol Int 58:227–231
14. Vervaet BA, D'Haese PC, De Broe ME, Verhulst A (2009) Crystalluric and tubular epithelial parameters during the onset of intratubular nephrocalcinosis: illustration of the 'fixed particle' theory in vivo. Nephrol Dial Transpl 24:3659–3668
15. Kumar V, Farell G, Yu S, Harrington S, Fitzpatrick L, Rzewuska E, Miller VM, Lieske JC (2006) Cell biology of pathologic renal calcification: contribution of crystal transcytosis, cell-mediated calcification, and nanoparticles. J Invest Med 54:412–424

16. Ryall RL (2011) The possible roles of inhibitors, promoters and macromolecules in the formation of calcium kidney stones. In: Rao N, Kavanagh JP, Preminger G (eds) Urinary tract stone disease. Springer, London, pp 31–60
17. Khan SR, Kok DJ (2004) Modulators of urinary stone formation. Front Biosci 9:1450–1482
18. Ryall RL (2004) Macromolecules and urolithiasis: parallels and paradoxes. Nephron Physiol 98:37–42
19. Kumar V, Yu S, Farell G, Toback FG, Lieske JC (2004) Renal epithelial cells constitutively produce a protein that blocks adhesion of crystals to their surface. Am J Physiol Renal Physiol 287:F373–F383
20. Lieske JC, Leonard R, Toback FG (1995) Adhesion of calcium oxalate monohydrate crystals to renal epithelial cells is inhibited by specific anions. Am J Physiol Renal Physiol 268:F604–F612
21. Kohjimoto Y, Ebisuno S, Tamura M, Ohkawa T (1996) Adhesion and endocytosis of calcium oxalate crystals on renal tubular cells. Scanning Microsc 10:459–470
22. Lieske JC, Toback FG (1993) Regulation of renal epithelial cell endocytosis of calcium oxalate monohydrate crystals. Am J Physiol Renal Physiol 264:F800–F807
23. Tsujihata M, Yoshimura K, Tsujikawa K, Tei N, Okuyama A (2006) Fibronectin inhibits endocytosis of calcium oxalate crystals by renal tubular cells. Int J Urol 13:743–746
24. Ebisuno S, Nishihata M, Inagaki T, Umehara M, Kohjimoto Y (1999) Bikunin prevents adhesion of calcium oxalate crystal to renal tubular cells in human urine. J Am Soc Nephrol 10(Suppl 14):S436–S440
25. Tei N, Tsujihata M, Tsujikawa K, Yoshimura K, Nonomura N, Okuyama A (2006) Hepatocyte growth factor has protective effects on crystal–cell interactions and crystal deposits. Urology 67:864–869
26. Verkoelen CF, Van Der Boom BG, Romijn JC (2000) Identification of hyaluronan as a crystal-binding molecule at the surface of migrating and proliferating MDCK cells. Kidney Int 58:1045–1054
27. Verkoelen CF, van der Boom BG, Houtsmuller AB, Schröder FH, Romijn JC (1998) Increased calcium oxalate monohydrate crystal binding to injured renal tubular epithelial cells in culture. Am J Physiol 274:F958–F965
28. Verhulst A, Asselman M, Persy VP, Schepers MS, Helbert MF, Verkoelen CF, De Broe ME (2003) Crystal retention capacity of cells in the human nephron: involvement of CD44 and its ligands hyaluronic acid and osteopontin in the transition of a crystal binding- into a non-adherent epithelium. J Am Soc Nephrol 14:107–114
29. Asselman M, Verhulst A, De Broe ME, Verkoelen CF (2003) Calcium oxalate crystal adherence to hyaluronan-, osteopontin-, and CD44-expressing injured/regenerating tubular epithelial cells in rat kidneys. J Am Soc Nephrol 14:3155–3166
30. Yamate T, Kohri K, Umekawa T, Amasaki N, Amasaki N, Isikawa Y, Iguchi M, Kurita T (1996) The effect of osteopontin on the adhesion of calcium oxalate crystals to Madin–Darby canine kidney cells. Eur Urol 30:388–393
31. Yamate T, Kohri K, Umekawa T, Iguchi M, Kurita T (1998) Osteopontin antisense oligonucleotide inhibits adhesion of calcium oxalate crystals in Madin–Darby canine kidney cell. J Urol 160:1506–1512
32. Yamate T, Kohri K, Umekawa T, Konya E, Ishikawa Y, Iguchi M, Kurita T (1999) Interaction between osteopontin on Madin Darby canine kidney cell membrane and calcium oxalate crystal. Urol Int 62:81–86
33. Sorokina EA, Wesson JA, Kleinman JG (2004) An acidic peptide sequence of nucleolin-related protein can mediate the attachment of calcium oxalate to renal tubule cells. J Am Soc Nephrol 15:2057–2065
34. Kumar V, Farell G, Deganello S, Lieske JC (2003) Annexin II is present on renal epithelial cells and binds calcium oxalate monohydrate crystals. J Am Soc Nephrol 14:289–297
35. Kohri K, Kodama M, Ishikawa Y, Katayama Y, Matsuda H, Imanishi M, Takada M, Katoh Y, Kataoka K, Akiyama T (1991) Immunofluorescent study on the interaction between collagen and calcium oxalate crystals in the renal tubules. Eur Urol 19:249–252
36. Asselman M, Verkoelen CF (2002) Crystal-cell interaction in the pathogenesis of kidney stone disease. Curr Opin Urol 12:271–276
37. Kramer G, Steiner GE, Prinz-Kashani M, Bursa B, Marberger M (2003) Cell-surface matrix proteins and sialic acids in cell–crystal adhesion; the effect of crystal binding on the viability of human CAKI-1 renal epithelial cells. Br J Urol 91:554–559
38. de Bruijn WC, Boevé ER, van Run PR, van Miert PP, de Water R, Romijn JC, Verkoelen CF, Cao LC, Schröder FH (1995) Etiology of calcium oxalate nephrolithiasis in rats. I. Can this be a model for human stone formation? Scanning Microsc 9:103–114
39. de Bruijn WC, Boevé ER, van Run PR, van Miert PP, Romijn JC, Verkoelen CF, Cao LC, Schröder FH (1994) Etiology of experimental cacluium oxalate monohydrate nephrolithiasis in rats. Scanning Microsc 8:541–549
40. de Water R, Noordermeer C, Houtsmuller AB, Nigg AL, Stijnen T, Schröder FH, Kok DJ (2000) The role of macrophages in nephrolithiasis in rats: an analysis of the renal interstitium. Am J Kidney Dis 36:615–625
41. de Water R, Leenen PJ, Noordermeer C, Nigg AL, Houtsmuller AB, Kok DJ, Schröder FH (2001) Cytokine production induced by binding and processing of calcium oxalate crystals in cultured macrophages. Am J Kidney Dis 38:331–338
42. de Water R, Nordermeer C, van der Kwast TH, Nizze H, Boevé ER, Kok DJ, Schröder FH (1999) Calcium oxalate nephrolithiasis: effect of renal crystal deposition on the cellular composition of the renal interstitium. Am J Kidney Dis 33:761–771
43. Schepers MS, Duim RA, Asselman M, Romijn JC, Schröder FH, Verkoelen CF (2003) Internalization of calcium oxalate crystals by renal tubular cells: a nephron segment-specific process? Kidney Int 64:493–500
44. Chauvet MC, Ryall RL (2005) Intracrystalline proteins and calcium oxalate crystal degradation in MDCK II cells. J Struct Biol 151:12–17
45. Grover PK, Thurgood LA, Fleming DE, van Bronswijk W, Wang T, Ryall RL (2008) Intracrystalline urinary proteins facilitate degradation and dissolution of calcium oxalate crystals in cultured renal cells. Am J Physiol Renal Physiol 294:F355–F361
46. Lieske JC, Swift H, Martin T, Patterson B, Toback FG (1994) Renal epithelial cells rapidly bind and internalize calcium oxalate monohydrate crystals. Proc Natl Acad Sci 91:6987–6991
47. Lieske JC, Norris R, Swift H, Toback FG (1997) Adhesion, internalization and metabolism of calcium oxalate monohydrate crystals by renal epithelial cells. Kidney Int 52:1291–1301
48. Lieske JC, Deganello S, Toback FG (1999) Cell-crystal interactions and kidney stone formation. Nephron 81:8–17
49. Lieske JC, Walsh-Reitz MM, Toback FG (1992) Calcium oxalate monohydrate crystals are endocytosed by renal epithelial cells and induce proliferation. Am J Physiol 262:F622–F630
50. Lieske JC, Toback FG, Deganello S (1998) Direct nucleation of calcium oxalate dihydrate crystals onto the surface of living renal epithelial cells in culture. Kidney Int 54:796–803
51. Ryall RL, Fleming DE, Grover PK, Chauvet M, Dean CJ, Marshall VR (2000) The hole truth: intracrystalline proteins and calcium oxalate kidney stones. Mol Urol 4:391–402
52. Ryall RL, Fleming DE, Doyle IR, Evans NA, Dean CJ, Marshall VR (2001) Intracrystalline proteins and the hidden ultrastructure

of calcium oxalate urinary crystals: implications for kidney stone formation. J Struct Biol 134:5–14
53. Ryall RL, Chauvet MC, Grover PK (2005) Intracrystalline proteins and urolithiasis: a comparison of the protein content and ultrastructure of urinary calcium oxalate monohydrate and dihydrate crystals. Br J Urol 96:654–663
54. Fleming DE, van Riessen A, Chauvet MC, Grover PK, Hunter B, van Bronswijk W, Ryall RL (2003) Intracrystalline proteins and urolithiasis: a synchrotron X-ray diffraction study of calcium oxalate monohydrate. J Bone Min Res 18:1282–1291
55. Wang T, Thurgood LA, Grover PK, Ryall RL (2010) A comparison of the binding of urinary calcium oxalate monohydrate and dihydrate crystals to human kidney cells in urine. Br J Urol Int 106:1768–1774
56. Lieske JC, Deganello S (1999) Nucleation, adhesion and internalization of calcium-containing urinary crystals by renal cells. J Am Nephrol Soc 10:S422–S429
57. Semangoen T, Sinchaikul S, Chen ST, Thongboonkerd V (2008) Altered proteins in MDCK renal tubular cells in response to calcium oxalate dihydrate crystal adhesion: a proteomics approach. J Proteome Res 7:2889–2896
58. Webber D, Chauvet MC, Ryall RL (2005) Proteolysis and partial dissolution of calcium oxalate: a comparative, morphological study of urinary crystals from black and white subjects. Urol Res 33:273–284
59. Chien YC, Masica DL, Gray JJ, Nguyen S, Vali H, McKee MD (2009) Modulation of calcium oxalate dihydrate growth by selective crystal-face binding of phosphorylated osteopontin and poly-aspartate peptide showing occlusion by sectoral (compositional) zoning. J Biol Chem 284:23491–23501
60. Thurgood LA, Cook AF, Sørensen ES, Ryall RL (2010) Face-specific incorporation of osteopontin into urinary and inorganic calcium oxalate monohydrate and dihydrate crystals. Urol Res 38:357–376
61. Thurgood LA, Wang T, Chataway TK, Ryall RL (2010) Comparison of the specific incorporation of intracrystalline proteins into urinary calcium oxalate monohydrate and dihydrate crystals. J Proteome Res 9:4745–4757
62. Shiraga H, Min W, VanDusen WJ, Clayman MD, Miner D, Terrell CH, Sherbotie JR, Foreman JW, Przysiecki C, Neilson EG, Hoyer JR (1992) Inhibition of calcium oxalate crystal growth in vitro by uropontin: another member of the aspartic acid-rich protein superfamily. PNAS 89:426–430
63. Asplin JR, Arsenault D, Parks JH, Coe FL, Hoyer JR (1998) Contribution of uropontin to inhibition of calcium oxalate crystallization. Kidney Int 53:194–199
64. Nishio S, Hatanaka M, Takeda H, Aoki K, Iseda T, Iwata H, Yokoyama M (2001) Calcium phosphate crystal-associated proteins: alpha-2-HS-glycoprotein, prothrombin fragment 1 and osteopontin. Int J Urol 8:S58–S62
65. Thurgood LA, Sorensen ES, Ryall RL (2011) The effect of intracrystalline and surface-bound osteopontin on the attachment of calcium oxalate dihydrate crystals to MDCKII cells in ultrafiltered human urine. Br J Urol (in press)
66. Kleinman JG, Wesson JA, Hughes J (2004) Osteopontin and calcium stone formation. Nephron Physiol 98:43–47
67. Okada A, Nomura S, Saeki Y, Higashibata Y, Hamamoto S, Hirose M, Itoh Y, Yasui T, Tozawa K, Kohri K (2008) Morphological conversion of calcium oxalate crystals into stones is regulated by osteopontin in mouse kidney. J Bone Miner Res 23:1629–1637
68. Hamamoto S, Nomura S, Yasui T, Okada A, Hirose M, Shimizu H, Itoh Y, Tozawa K, Kohri K (2010) Effects of impaired functional domains of osteopontin on renal crystal formation: analyses of OPN-transgenic and OPN-knockout mice. J Bone Miner Res 25:2436–2447
69. Senger DR, Perruzzi CA, Papadopoulos A, Tenen DG (1989) Purification of a human milk protein closely similar to tumor-secreted phosphoproteins and osteopontin. Biochim Biophys Acta 996:43–48
70. Christensen B, Nielsen MS, Haselmann KF, Petersen TE, Sørensen ES (2005) Post-translationally modified residues of native human osteopontin are located in clusters: identification of 36 phosphorylation and five O-glycosylation sites and their biological implications. Biochem J 390:285–292
71. Bautista DS, Denstedt JM, Chamber AF, Harris JF (1996) Low-molecular-weight variants of osteopontin generated by serine proteinases in urine of patients with kidney stones. J Cell Biochem 61:402–409
72. Thurgood LA, Grover PK, Ryall RL (2008) High calcium concentration and calcium oxalate crystals cause significant inaccuracies in the measurement of urinary osteopontin by enzyme linked immunosorbent assay. Urol Res 36:103–110
73. Ryall RL, Grover PK, Thurgood LA, Chauvet MC, Fleming DE, van Bronswijk W (2007) The importance of a clean face: the effect of different washing procedures on the association of Tamm-Horsfall glycoprotein and other urinary proteins with calcium oxalate crystals. Urol Res 35:1–14
74. Verkoelen CF, van der Boom BG, Kok DJ, Houtsmuller AB, Visser P, Schröder FH, Romijn JC (1999) Cell type-specific acquired protection from crystal adherence by renal tubule cells in culture. Kidney Int 55:1426–1433
75. Grover PK, Thurgood LA, Ryall RL (2007) Effect of urine fractionation on attachment of calcium oxalate crystals to renal epithelial cells: implications for studying renal calculogenesis. Am J Physiol Renal Physiol 292:F1396–F1403
76. Walton RC, Kavanagh JP, Heywood BR (2003) The density and protein content of calcium oxalate crystals precipitated from human urine: a tool to investigate ultrastructure and the fractional volume occupied by organic matrix. J Struct Biol 143:2–14
77. Belliveau J, Griffin H (2001) The solubility of calcium oxalate in tissue culture media. Anal Biochem 291:69–73
78. Grover PK, Thurgood LA, Wang T, Ryall RL (2010) The effects of intracrystalline and surface-bound proteins on the attachment of calcium oxalate monohydrate crystals to renal cells in undiluted human urine. Br J Urol 105:708–715
79. Hsu WL, Lin MJ, Hsu JP (2009) Dissolution of solid particles in liquids: a shrinking core model. World Acad Sci Eng Technol Chem Mater Eng 2:4–8
80. Addadi L, Joester D, Nudelman F, Weiner S (2006) Mollusk shell formation: a source of new concepts for understanding biomineralization processes. Chemistry 12:980–987
81. Qiu SR, Orme CA (2008) Dynamics of biomineral formation at the near-molecular level. Chem Rev 108:4784–4822
82. Fleming DE (2004) Urolithiasis: occurrence and function of intracrystalline proteins in calcium oxalate monohydrate crystals. Dissertation, Curtin University of Technology, Western Australia. http://espace.library.curtin.edu.au/R?func=search-simple-go&ADJACENT=Y&REQUEST=adt-WCU20050124.093851
83. White DJ, Coyle-Rees M, Nancollas GH (1988) Kinetic factors influencing the dissolution behaviour of calcium oxalate stones: a constant composition study. Calcif Tissue Int 43:319–327
84. Lepage L, Tawashi R (1982) Growth and characterization of calcium oxalate dihydrate crystals (weddellite). J Pharm Sci 71:1059–1062
85. Harrell PC, McCawley LJ, Fingleton B, McIntyre JO, Matrisian LM (2005) Proliferative effects of apical, but not basal, matrix metalloproteinase-7 activity in polarized MDCK cells. Exp Cell Res 303:308–320
86. McGwire GB, Becker RP, Skidgel RA (1999) Carboxypeptidase M, a glycosylphosphatidylinositol-anchored protein, is localized

on both the apical and basolateral domains of polarized Madin-Darby canine kidney cells. J Biol Chem 274:31632–31640
87. Gstraunthaler G, Pfaller W, Kotanko P (1985) Biochemical characterization of renal epithelial cell cultures (LLC-PK1 and MDCK). Am J Physiol 248:F536–F544
88. Hackett RL, Shevock PN, Khan SR (1994) Madin-Darby canine kidney cells are injured by exposure to oxalate and to calcium oxalate crystals. Urol Res 22:197–204
89. Richardson JC, Scalera V, Simmons NL (1981) Identification of two strains of MDCK cells which resemble separate nephron tubule segments. Biochim Biophys Acta 673:26–36
90. Oliveira V, Ferro ES, Gomes MD, Oshiro ME, Almeida PC, Juliano MA, Juliano L (2000) Characterization of thiol-, aspartyl-, and thiol-metallo-peptidase activities in Madin-Darby canine kidney cells. J Cell Biochem 76:478–488
91. Shalamanova L, Kübler B, Scharf JG, Braulke T (2001) MDCK cells secrete neutral proteases cleaving insulin-like growth factor-binding protein-2 to -6. Am J Physiol Endocrinol Metab 281:E1221–E1229
92. Andersson G, Ek-Rylander B, Hollberg K, Ljusberg-Sjölander J, Lång P, Norgård M, Wang Y, Zhang SJ (2003) TRACP as an osteopontin phosphatase. J Bone Miner Res 18:1912–1915
93. Christensen B, Schack L, Kläning E, Sørensen ES (2010) Osteopontin is cleaved at multiple sites close to its integrin-binding motifs in milk and is a novel substrate for plasmin and cathepsin D. J Biol Chem 285:7929–7937
94. Agnihotri R, Crawford HC, Haro H, Matrisian LM, Havrda MC, Liaw L (2001) Osteopontin, a novel substrate for matrix metalloproteinase-3 (stromelysin-1) and matrix metalloproteinase-7 (matrilysin). J Biol Chem 276:28261–28267
95. Moriyama MT, Domiki C, Miyazawa K, Tanaka T, Suzuki K (2005) Effects of oxalate exposure on Madin-Darby canine kidney cells in culture: renal prothrombin fragment-1 mRNA expression. Urol Res 33:470–475
96. Hartz PA, Wilson PD (1997) Functional defects in lysosomal enzymes in autosomal dominant polycystic kidney disease (ADPKD): abnormalities in synthesis, molecular processing, polarity, and secretion. Biochem Mol Med 60:8–26
97. Neame PJ, Butler WT (1996) Post-translational modification in rat bone osteopontin. Connect Tissue Res 35:145–150
98. Christensen B, Kazanecki CC, Petersen TE, Rittling SR, Denhardt DT, Sørensen ES (2007) Cell type-specific post-translational modifications of mouse osteopontin are associated with different adhesive properties. J Biol Chem 282:19463–19472
99. Kasemo B, Lausmaa J (1994) Material-tissue interfaces: the role of surface properties and processes. Environ Health Perspect 102(Suppl 5):41–45
100. Malmström J, Shipovskov S, Christensen B, Sørensen ES, Kingshott P, Sutherland DS (2009) Adsorption and enzymatic cleavage of osteopontin at interfaces with different surface chemistries. Biointerphases 4:47–55
101. Nishiyama K, Sugawara K, Nouchi T, Kawano N, Soejima K, Abe S, Mizokami H (2008) Purification and cDNA cloning of a novel protease inhibitor secreted into culture supernatant by MDCK cells. Biologicals 36:122–133
102. Kon S, Ikesue M, Kimura C, Aoki M, Nakayama Y, Saito Y, Kurotaki D, Diao H, Matsui Y, Segawa T, Maeda M, Kojima T, Uede T (2008) Syndecan-4 protects against osteopontin-mediated acute hepatic injury by masking functional domains of osteopontin. J Exp Med 205:25–33
103. Shanmugam V, Chackalaparampil I, Kundu GC, Mukherjee AB, Mukherjee BB (1997) Altered sialylation of osteopontin prevents its receptor-mediated binding on the surface of oncogenically transformed TSB77 cells. Biochem 36:5729–5738
104. Kugler P, Wolf G, Scherberich J (1985) Histochemical demonstration of peptidases in the human kidney. Histochem 83:337–341
105. Singh AK (1993) Presence of lysosomal enzymes in the normal glomerular basement membrane matrix. Histochem J 25: 562–568
106. Yokota S, Tsuji H, Kato K (1985) Immunocytochemica localization of cathepsin D in lysosomes of cortical collecting tubule cells of the rat kidney. J Histochem Cytochem 33:191–200
107. ATCC (2011) ATCC catalogue search. http://www.atcc.org/ATCCAdvancedCatalogSearch/ProductDetails/tabid/452/Default.aspx?ATCCNum=CRL-2936&Template=cellBiology. Accessed 16 March 2011
108. Huang HS, Chen CF, Chien CT, Chen J (2000) Possible biphasic changes of free radicals in ethylene glycol-induced nephrolithaisis in rats. BJU Int 85:1143–1149
109. Baggio B, Gambaro G, Ossi E, Favaro S, Borsatti A (1983) Increased urinary excretion of renal enzymes in idiopathic calcium oxalate nephrolithiasis. J Urol 129:1161–1162